

 Open access • Posted Content • DOI:10.1101/507467

The MHC class-II HLA-DR receptor mediates bat influenza A-like H17N10 virus entry into mammalian cells — [Source link](#)

Efstathios S. Giotis, George Carnell, George Carnell, Erik F. Young ...+5 more authors

Institutions: Imperial College London, Medway School of Pharmacy, University of Cambridge, Columbia University ...+1 more institutions

Published on: 04 Jan 2019 - bioRxiv (Cold Spring Harbor Laboratory)

Topics: Neuraminidase, Viral entry, HLA-DR, MHC class II and Virus

Related papers:

- [Entry of the bat influenza H17N10 virus into mammalian cells is enabled by the MHC class II HLA-DR receptor.](#)
- [Sequence dynamics of three influenza A virus strains grown in different MDCK cell lines, including those expressing different sialic acid receptors.](#)
- [Analysis of hemagglutinin-mediated entry tropism of H5N1 avian influenza](#)
- [Enhanced Human-Type Receptor Binding by Ferret-Transmissible H5N1 with a K193T Mutation.](#)
- [Mammalian Adaptive Mutations of the PA Protein of Highly Pathogenic Avian H5N1 Influenza Virus](#)

Share this paper:    

View more about this paper here: <https://typeset.io/papers/the-mhc-class-ii-hla-dr-receptor-mediates-bat-influenza-a-39xgqhre5o>

1 **The MHC class-II HLA-DR receptor mediates bat influenza A-like H17N10 virus entry**
2 **into mammalian cells**

3 **Efstathios S Giotis^{1*}, George Carnell^{2,3}, Erik F. Young^{4†}, Saleena Ghanny^{4††}, Patricia**
4 **Soteropoulos^{4††}, Wendy S Barclay¹, Michael A Skinner¹, Nigel Temperton²**

5 ¹Section of Virology, Department of Medicine, St Mary's Campus, Imperial College London, UK.

6 ²Viral Pseudotype Unit, Medway School of Pharmacy, University of Kent and University of
7 Greenwich, Chatham Maritime, UK.

8 ³Laboratory of Viral Zoonotics, Department of Veterinary Medicine, University of Cambridge,
9 UK.

10 ⁴Hackensack University Medical Centre Department of Surgery, Hackensack, NJ.

11

12 Current affiliations:

13 [†]Bioelectronic Systems Lab, Columbia University, NY, USA.

14 ^{††}University of Medicine and Dentistry of New Jersey, Centre for Applied Genomics, Newark,
15 NJ, USA.

16

17 *Corresponding author: Efstathios S Giotis e.giotis@imperial.ac.uk

18

19 **Abstract:**

20 Bats are notorious reservoirs of diverse, potentially zoonotic viruses, exemplified by the
21 evolutionarily distinct, influenza A-like viruses H17N10 and H18N11 (BatIVs). The surface
22 glycoproteins [haemagglutinin (H) and neuraminidase (N)] of BatIVs neither bind nor cleave
23 sialic acid receptors, which suggests that these viruses employ cell attachment and entry
24 mechanisms that differ from those of classical influenza A viruses (IAVs). Identifying the
25 cellular factors that mediate entry and determine susceptibility to infection will help assess
26 the host range of BatIVs. Here, we investigated a range of cell lines from different species for

27 their susceptibility to infection by pseudotyped viruses (PV) bearing bat H17 and/or N10
28 envelope glycoproteins. We show that a number of human haematopoietic cancer cell lines
29 and the canine kidney MDCK II (but not MDCK I) cells are susceptible to H17-pseudotypes
30 (H17-PV). We observed with microarrays and qRT-PCR that the dog leukocyte antigen DLA-
31 DRA mRNA is over expressed in late passaged parental MDCK and commercial MDCK II cells,
32 compared to early passaged parental MDCK and MDCK I cells, respectively. The human
33 orthologue HLA-DRA encodes the alpha subunit of the MHC class II HLA-DR antigen-binding
34 heterodimer. Small interfering RNA- or neutralizing antibody-targeting HLA-DRA, drastically
35 reduced the susceptibility of Raji B cells to H17-PV. Conversely, over expression of HLA-DRA
36 and its paralogue HLA-DRB1 on the surface of the unsusceptible HEK293T/17 cells conferred
37 susceptibility to H17-PV. The identification of HLA-DR as an H17N10 entry mediator will
38 contribute to a better understanding of the tropism of the virus and will elucidate its zoonotic
39 transmission.

40
41 **Keywords:** influenza, bats, pseudotype virus, MHC-class II, HLA-DR

42
43 **Abbreviations:** SARS: severe acute respiratory syndrome; MERS: Middle-East respiratory
44 syndrome; CoV: coronavirus; MDCK: Madin-Darby canine kidney cells; HIV: human
45 immunodeficiency virus; CD4: cluster of differentiation 4; MHC: Major histocompatibility
46 complex; ATCC: American type culture collection; gag: group-specific antigen; pol:
47 polymerase; SEM: standard error of the mean.

48
49 **Main:**
50 Outbreaks of SARS, MERS, Nipah and Ebola have highlighted the critical need to focus on the
51 zoonotic potential of known, and novel, bat viruses to improve forecasting, prevention and
52 control of epidemics. Viral diversity in bats is exemplified by the discovery of the enigmatic

53 influenza A-like viruses (BatIVs) H17N10 and H18N11 in asymptomatic New World bats
54 (*Sturnira lilium* and *Artibeus planirostris* respectively)^{1,2} and more recently by the detection of
55 a virus related to avian H9N2 in Egyptian *Rousettus aegyptiacus* bats³. Such discoveries
56 prompted investigation of the pandemic potential of these viruses and led to concern that bats
57 may be a neglected reservoir of novel influenza viruses⁴.

58 Influenza A viruses (IAVs) are enveloped orthomyxoviruses with eight single-stranded
59 negative-sense viral RNAs (vRNAs) encapsidated into viral ribonucleoproteins (vRNPs). The
60 original source of classical IAVs is aquatic birds, from which they emerge, *via* genome
61 reassortment and mutation, to cause sporadic pandemics in humans, lower animals and other
62 birds^{5, 6}. They are classified into different subtypes based on their envelope glycoproteins
63 (trimeric haemagglutinin, HA: H1-H18, and tetrameric neuraminidase, NA: N1-N11)⁷. HA is
64 synthesised as a precursor protein in infected cells and its cleavage by host cell proteases sets
65 in motion a complex series of events that is initiated by receptor binding and is terminated
66 with the penetration of the virus into the cytoplasm of target cells⁸. HA conventionally
67 attaches to host-specific sialic acid (SA) moieties⁶. These are terminal sugars of larger
68 carbohydrate chains attached to the cell membrane by the lipids or proteins that they
69 decorate. When HA attaches to them, it triggers endocytosis of the virus into membrane
70 bound endosomes^{9, 10}. Acidification of the endosome induces conformational changes to HA,
71 which lead sequentially to: insertion of the hydrophobic “HA fusion peptide” into the host
72 membrane, juxtaposition of the viral and endosomal membranes and subsequent release of
73 the vRNPs into the cytoplasm via a fusion pore^{11, 12}. In contrast, NAs are glycosidases which
74 primarily cleave cell surface SA and therefore facilitate the release and spread of virus
75 progeny upon egress, as well as disaggregation of virions before entry^{13, 14}.

76 The crystal structures of BatIV HAs and NAs revealed divergence of their protein
77 conformations from those of conventional IAVs, suggesting distinct binding and functional
78 properties^{2, 15, 16, 17}. Bat H17 and H18 proteins have typical HA folds but lack an obvious cavity

79 to accommodate SA^{2, 15, 17}. The cell receptors for the BatIVs are as yet unidentified, but they
80 are clearly not SA moieties, a conclusion reached by several studies^{15, 18, 19}. Furthermore, bat
81 N10 and N11 are structurally similar to classical NAs but lack conserved amino acids for SA
82 binding and cleavage^{2, 16, 17} and do not exhibit typical neuraminidase activity^{18, 20}. Initial
83 efforts to isolate infectious BatIVs directly from bats have failed, mainly because the receptors
84 were unknown and susceptible cell lines were unavailable^{21, 22, 23}. Attempts to circumvent
85 these limitations have included H17- or H18-pseudotyped vesicular stomatitis virus (VSV^{19,}
86 ²⁴), engineered BatIV/IAV chimeric viruses^{23, 25}, and authentic BatIVs reconstructed using
87 reverse genetics²⁶. H17-VSV was able to infect bat cell lines (EidNi, HypNi, and EpoNi) but
88 only a few, common cell lines of flightless mammals, including some of human (U-87 MG
89 glioblastoma and SK-Mel-28 melanoma) and canine (RIE1495 and MDCK II kidney) origin^{19, 24,}
90 ²⁶. These cells could also be infected with reconstructed H17N10 and H18N11 viruses²⁶. The
91 ability of BatIVs to infect mammalian cell lines *in vitro*, and their unconventional features,
92 raised concerns about their zoonotic and epidemic potential. Identifying the BatIV cell surface
93 receptors and delineating the mechanistic basis of the host-virus interaction are key to
94 assessing their potential host range and public health significance.

95
96 HIV-1 derived-pseudotypes bearing heterologous envelope proteins (PV) have been used
97 widely for the assessment of cellular tropism and the identification of cellular receptors or
98 attachment factors for a range of viruses^{27, 28, 29, 30, 31}. Such pseudotypes have proved a
99 reliable model to study the capacity of H17N10 for entry into various cell lines^{27, 32}. Using this
100 approach, we have shown that H17-PV, and H17N10-PV (A/little yellow-shouldered
101 bat/Guatemala/060/2011) are recovered from producer HEK293T/17 cells exclusively in the
102 presence of the human airway trypsin-like protease (HAT) or the transmembrane protease,
103 serine 2 (TMPRSS2) (Fig. 1a)³². In this study, a panel ($n=35$; Supplementary material 1) of cell
104 lines from different tissues and species were challenged with H17- and/or N10-PV to study

105 the distribution of the H17N10 receptor(s) (Fig. 1b). Efficiency of infections with PV was
106 quantified (after 48 h) by the expression of a firefly luciferase (FLuc) reporter gene encoded
107 by the lentiviral genome. Parallel infections were conducted with PV bearing either classical
108 H5 (H5-PV; A/Vietnam/1194/2004; H5N1 clade 1) or VSV-G (VSV-G-PV) glycoproteins (the
109 latter displaying very broad tropism) as positive controls to eliminate possible post-binding
110 blockage factors. HIV particles produced in the absence of a viral envelope protein (Δ -env)
111 served as a negative control. H17-PV displayed highly limited host and species cell tropism,
112 suggesting that the H17 cellular receptor(s) are not ubiquitous (Fig. 1b). Of note, the bat cell
113 lines (lung & kidney) from *S. lilium* in which H17N10 was discovered, were not susceptible to
114 PV. This implies that expression of the H17-putative receptor(s) and/or viral entry-related
115 host factors was either lost during immortalisation or is tissue-type restricted. Conversely, we
116 show that the dog epithelial kidney MDCK II (unlike MDCK I) cells are susceptible to H17-PV
117 with titers comparable to those of control VSV-G- and H5-PV in the range of 10^6 to 10^7
118 RLU/ml (Fig. 1c). They were not susceptible to PV expressing N10 alone and co-expression of
119 N10 with H17 did not improve infection of MDCK II (Fig. 1c), which suggests that N10 has a
120 dispensable role in viral entry (*in vitro*). To characterise the H17 putative receptors, MDCK II
121 cells were either pre-treated with neuraminidase, tunicamycin or pronase or treated with
122 ammonium chloride before infection with H17-PV. Infectivity with H17- and H5-PVs, as well
123 as cytotoxicity (by trypan blue exclusion), were assayed 24 h post treatment (Fig. 1d). Pre-
124 treatment of MDCK II cells with neuraminidase from *Clostridium perfringens* (1-100 mU), which
125 cleaves cell surface SA, reduced H5-PV infection by 68-86% but did not significantly affect
126 infection by H17-PV, supporting the notion that SA are not the cell surface receptors for
127 H17^{19, 26}. Classical IAVs primarily enter cells via endocytosis followed by endosomal fusion
128 triggered by low pH. Treatment of MDCK II cells with the pH neutralising agent ammonium
129 chloride (1-100 mM) abolished luciferase activity for both H5- and H17-PV, demonstrating
130 that entry of H17, like IAVs, into target cells is pH-dependent. Similar results were obtained in

131 RIE1495 cells³². Entry of H17-PV was more susceptible to pre-treatment of MDCK II cells with
132 proteases or tunicamycin (an inhibitor of *N*-glycosylation) than was entry of H5-PV (being
133 reduced by up to 72 and 78%, compared to 45 and 20%, respectively), suggesting that the
134 H17-cellular receptor(s) may be a glycosylated protein, in line with previous proposals¹⁹.

135

136 MDCK I and II represent early and late passaged cells from the same parental NBL-2 cell line
137 (CCL-34, ATCC). MDCK are valuable cell lines in studies of viruses, cell-cell junctions and
138 epithelial differentiation but consist of heterogeneous cell populations and their phenotypes
139 vary significantly between user laboratories³³. In addressing the factors that permit infection
140 of H17-PV in late passaged MDCK II cells, we considered that parental NBL-2 cells undergo
141 passage number-dependent phenotypic changes that may be reflected at transcriptional level.
142 The phenotypic transition of NBL-2 cells to early and late MDCK cells was investigated using
143 the Affymetrix canine microarray 2.0 (E-GEOD-14837; passages 8 and 21 respectively). The
144 microarray analysis identified 17 differentially regulated transcripts: 12 up-regulated and 5
145 down-regulated in late- compared to early-passaged cells (Fig. 2a). The current prevalent
146 hypothesis is that single or multiple cell surface molecules are essential for the initial
147 attachment and uptake of enveloped viruses into cells^{34, 35}. Therefore, we surveyed the
148 differentially regulated transcripts for encoded, surface-anchored proteins using a combined
149 analysis of: available Gene Ontology annotations, existing literature as well as transmembrane
150 protein domain and subcellular localisation prediction algorithms (Phobius, TMHMM and
151 DeepLoc). The analysis identified the dog leukocyte antigen class II DR α -chain (DLA-DRA) as
152 the only transcript, encoding a membrane protein, over-expressed in late, compared to early,
153 passage MDCK cells (full data in Supplementary material 2). Significant over-expression of
154 DLA-DRA (and its paralogue DLA-DRB1) was also confirmed (by qRT-PCR) in MDCK II
155 compared to MDCK I cells (Fig. 2b).

156

157 DLA-DRA is a well-conserved orthologue of the human leukocyte antigen class II DR α -chain
158 (HLA-DRA) (~90% amino acid identity between canine, human and *Desmodus rotundus* bat
159 ectodomains; Supplementary material 3). In humans, MHC-II molecules occur as three highly
160 polymorphic isotypes (HLA-DR, HLA-DP and HLA-DQ) which are selectively expressed
161 under normal conditions on the surface of antigen presenting cells (APCs), including B,
162 dendritic and mononuclear phagocyte cells. These molecules are non-covalently associated
163 heterodimers of two glycosylated, transmembrane polypeptide chains, the monomorphic
164 35-kDa α -chain and the highly polymorphic 28-kDa β -chain³⁶. Both chains have an
165 extracellular portion composed of two domains (α 1 and α 2, or β 1 and β 2) that is anchored
166 on the cell membrane by short transmembrane and cytoplasmic domains (Fig. 2c). In the
167 classical scenario, the protease-derived foreign antigen peptides bind to MHC class II proteins
168 in the cleft formed by the α 1 and β 1 domains, and the complex is transported to the cell
169 surface^{36, 37}. When antigenic peptides are not available, endogenous peptides such as the class
170 II associated invariant peptide (CLIP) substitute them and restore MHC class II dimer
171 stability³⁷. The complex of HLA-DR and endocytosed peptides (usually 9-30 amino acids in
172 length), constitutes a ligand for the T-cell receptor (TCR) and plays a key role in the
173 presentation of foreign antigens to CD4⁺ T helper cells and immune surveillance^{38, 39}.

174

175 Since the ultimate goal of our studies is to obtain insight on the zoonotic potential of H17N10,
176 we focused on the possible influence of HLA-DR on cellular susceptibility to H17. Hence,
177 taking advantage of the high expression of HLA-DR on certain human hematopoietic
178 carcinomas⁴⁰, we further explored H17-PV tropism using a panel of human leukaemia and
179 lymphoma cell lines (Fig. 2d). We found that the Burkitt's lymphoma-derived Raji, Ramos and
180 BJAB B-lymphocytes and the B lymphoblastoid cells (B-LCL) show decreasing susceptibility,
181 in that order, to H17-PV. Kasumi-1 leukaemic cells showed marginal susceptibility in terms of
182 luciferase activity, while Molt-4 and HL-60 leukaemic cells, Jurkat T-cells, pro-monocytic THP-

183 1 and U-937 cells, and primary B cells showed no susceptibility to the pseudotypes (Fig. 2d,
184 left Y axis). We hypothesised that the different susceptibility of the various cell types by H17-
185 PV were due to disparate expression of HLA-DR, confirmed by qRT-PCR analysis for a non-
186 polymorphic region of the α chain of HLA-DR on the same samples (Fig. 2d, right Y-axis). The
187 presence of the HLA-DR heterodimer was also confirmed by flow cytometry with a FITC-
188 conjugated monoclonal antibody (clone Tü36), which specifically binds to a monomorphic
189 epitope on the HLA-DR α/β complex and not the isolated α or β chains (Fig. 2e)⁴¹. Both
190 approaches indicate association between mRNA levels, the surface expression of HLA-DR
191 heterodimer and susceptibility to H17-PV. Raji, BJAB and Ramos B cells were found to consist
192 of 100% HLA-DR⁺ cells; Kasumi-1 demonstrated a 7% subpopulation of HLA-DR⁺ cells and
193 MOLT-4 and HL-60 cells were 100% HLA-DR⁻. These results were relatively constant and did
194 not change with factors such as cell density or passage number.

195

196 To confirm the influence of HLA-DR on H17-PV entry into B cells, HLA-DR was independently
197 suppressed by siRNA-mediated inhibition or by antibody blocking. Raji B cells were
198 transfected twice over 48 h with an siRNA mixture specific for HLA-DRA (siHLA-DRA) or a
199 control siRNA (siControl) and then challenged with the H17-PV for another 48 h. The
200 efficiency of HLA-DRA knock-down was confirmed by qRT-PCR and western Blot. The mRNA
201 and protein expression of HLA-DRA was reduced by $\geq 50\%$ in Raji cells transfected with
202 siHLA-DRA compared to those transfected with siControl. Knocking down HLA-DRA in Raji
203 cells correspondingly reduced the infection of H17-PV by 50% (Fig. 2f).

204

205 To determine if blocking attachment of virus to the HLA-DR ectodomain can prevent its entry,
206 Raji cells were incubated with increasing concentrations of a monoclonal antibody (mAb
207 Clone 302CT2.3.2) targeting a monomorphic, extracellular region of the HLA-DRA antigen

208 (HLA-DRA epitope: amino acids 48-75). The presence of the antibody significantly reduced, in
209 a dose-dependent manner, infection with H17-PV but not VSV-G-PV (Fig. 2g).

210

211 We next sought to ascertain whether ectopic expression of HLA-DR was sufficient to increase
212 the susceptibility of non-APC, HEK293T/17, cells to the H17-PVs. HEK293T/17 cells were
213 transiently transfected with the DRA expression vector, alone or in combination with DRB1.
214 Surface expression of the α/β heterodimer was validated using immunofluorescence and flow
215 cytometry. Expression of either DRA or DRB1 alone resulted in marginal or no increase in
216 surface staining of HLA-DR or H17-PV infection (data not shown). In contrast, 1:1 co-
217 expression of both DRA and DRB1 formed a functional α/β heterodimer on the cell surface in
218 approximately 47% of the cell population (Fig. 2h and Supplementary material 4). This
219 suggests that both α and β chains are necessary for cell-surface expression, consistent with
220 previous studies^{42, 43}. Transient over expression of HLA-DR in HEK293T/17 cells resulted in
221 significant infection by H17-PV. Infection was higher by more than two orders of magnitude
222 (Fig. 2i) in Fluorescence-activated cell sorting (FACS)-sorted cells enriched for HLA-DR.
223 Further, expression of the human HLA-DR α and β chains in the bat *Pteropus alecto* kidney
224 PakiTO3 cells allowed infection with H17-PV (Supplementary material 5).

225

226 Taken together, HLA-DR is shown to function as a *bona fide* entry mediator for H17 but may
227 function with unknown factors that facilitate virus internalisation. Interaction between HLA-
228 DR and H17 may trigger viral entry through canonical receptor-mediated endocytosis, but
229 could also trigger entry through an activation of cell signalling pathways that the virus
230 subverts to its advantage. Our finding therefore raises questions on the utility and possible
231 evolutionary advantage(s) that an APC-associated receptor would confer to H17N10
232 infectivity and broader fitness. Some viruses exploit cells of the immune system, such as
233 macrophages, B and dendritic cells, either as viral reservoirs or as “Trojan horses” to

234 penetrate the epithelial barriers^{44, 45}. The measles virus for example, exploits macrophages or
235 dendritic cells, which traffic the virus to bronchus-associated lymphoid tissue or regional
236 lymph nodes, resulting in local amplification and subsequent systemic dissemination by
237 viremia⁴⁶. A similar strategy employed by H17N10 could provide an explanation on why viral
238 RNA was detected in different organs and tissues in carrier *S. liliu* bats (i.e. lung, kidney,
239 liver, intestine) and why the virus fails to grow *in vitro* in cell lines developed from the same
240 tissues^{1, 26}. The prototypic gammaherpesvirus, Epstein-Barr virus (EBV), employs resting B
241 cells as transfer vehicles for infection of epithelial cells⁴⁷, and also uses the HLA-DR (β 1
242 domain) as receptor in order both to enter B cells as well as to impair antigen presentation
243 (by sterically blocking the engagement of HLA-DR1 and the TCR V α domain)^{48, 49, 50}. It is
244 possible that through efficient binding to HLA-DR, H17N10 may have developed a means of
245 simultaneously accessing lymphoid cells and blocking T-cell responses. Such an immune
246 evasion mechanism could explain, at least partially, its survival and asymptomatic status in
247 carrier bats. With limited functional information available on the bat MHC-II, the biological
248 role of the host HLA-DR orthologue in the pathogenesis and transmission mechanisms of the
249 H17N10 virus remains obscure.

250 In this study we did not establish the stoichiometry of the HLA-DR: H17 engagement, or
251 clarify how the virus moves to sub-membranous regions and might hijack the receptor-
252 mediated signalling pathway to promote its internalization. It is likely that the determinants
253 of viral entry *in vivo* are more complicated. We cannot rule out the use by H17N10 (as by
254 other bat-borne viruses, *e.g.* SARS CoV^{51, 52}) of more than one molecular species as (co-)
255 receptors. Nevertheless, the implication of this study is that H17N10 has the capacity to
256 enter human HLA-DR⁺ cells and our work provides substantial evidence that the H17N10
257 virus has zoonotic potential. The current finding not only sheds light on the understanding
258 of BatIV host range, but also provides additional information on the evolution of influenza
259 A viruses.

260

261 **Materials and methods**

262 **Cell lines, cell culture and treatment**

263 Cell lines (complete description in Supplementary material 1) were kindly provided as
264 follows: the HEK293T/17 cells were provided by Dr Edward Wright (University of
265 Westminster, UK); Kasumi-1, HL-60, Molt-4, Jurkat cells from Professor Paul Farrell (Imperial
266 College London, UK); *Pteropus alecto* cell lines from Professor Linfa Wang (NUS Duke,
267 Singapore); *Sturnira lilium*, *Artibeus planirostris*, and *Carolia perspicillata* cell lines have been
268 generated in the labs of Dr Carles Martínez-Romero/Professor Adolfo Garcia-Sastre (Icahn
269 School of Medicine, New York) from bat tissue samples originally collected by Dr Eugenia
270 Corrales-Aguilar (University of Costa Rica); B-LCL were created by Dr Konstantinos Paschos
271 by infecting with recombinant EBV B cells from isolated peripheral blood monocytes (PBMCs)
272 of a healthy donor of the prototypical B95-8 background (Imperial College London); Raji,
273 Ramos and BJAB from Dr Rob White (Imperial College London); U-937 and THP-1, BEAS-2B,
274 Caco-2 from Dr Marcus Dorner, Dr Michael Edwards and Professor Robin Shattock
275 respectively (Imperial College London). The rest of cell lines were either from the collection of
276 Dr Michael Skinner or from ATCC. Primary B cells were a kind gift by Dr Rob White (Imperial
277 College London). B cells were isolated from peripheral blood leukocyte (PBL) samples
278 obtained from anonymous buffy coat donors (UK Blood Transfusion Service) by
279 centrifugation over Ficoll. CD19 microbeads were used for magnetic separation of purified B
280 cells using an autoMACS separator (Miltenyi Biotec). All cell lines in this study were cultured
281 according to standard mammalian tissue culture protocols (ATCC; www.atcc.org). Bat cell
282 lines were propagated in Dulbecco's modified eagle medium (DMEM) (Life Technologies)
283 supplemented with heat-inactivated 15% fetal bovine serum (Life Technologies), penicillin
284 (100 U/ml) and streptomycin (100 µg/ml; Invitrogen). All cells were maintained in a

285 humidified incubator at 37°C and 5% CO₂ and were found free of mycoplasma contamination
286 on repeated testing with the MycoFluor Mycoplasma Detection Kit (Life Technologies, UK).
287 MDCK II cells were treated as previously¹⁹ with the following modifications. MDCK II cells
288 were either treated with the endosomal acidification reagent ammonium chloride (1, 10 or
289 100 mM), or pre-treated with neuraminidase from *Clostridium perfringens* for 2 h (1, 10 or 100
290 mM) or pronase (a mixture of endo- and exoproteases from *Streptomyces griseus* at a final
291 concentration of 5, 10 or 50 µg/ml; Calbiochem, UK) for 30 min, an N-glycosylation inhibitor
292 (tunicamycin from *Streptomyces* sp. at a final concentration of 0.01, 0.1 or 1 µg/ml; Sigma-
293 Aldrich, UK) for 5 h. Pre-treated cells were washed with phosphate buffer saline (PBS) 3
294 times, and then incubated/infected as before with PVs for another 24 h. Cell viabilities were
295 assessed by a trypan blue exclusion test.

296

297 **Lentiviral pseudotype virus production and susceptibility assays**

298 Pseudotypes expressing H17 and N10 genes were produced as described previously^{32, 53}.
299 Briefly, the lentiviral packaging plasmid p8.91⁵⁴, the pCSFLW firefly luciferase lentiviral
300 vector⁵⁵ or the GFP expressing vector pCSGW, the expression plasmids for H17 and/or N10
301 [vector pl.18⁵⁶ and the protease encoding plasmid pCAGGS-HAT (a kind gift by Eva Böttcher-
302 Friebertshäuser, Philipps University of Marburg, Germany) were co-transfected using
303 polyethylenimine transfection reagent (Sigma Aldrich, UK) into HEK293T/17 cells, plated on
304 6-well Nunclon[®] plates (Thermo Fisher Scientific, UK). Supernatants were collected 48-72 h
305 post transfection and filtered through a 0.45 µm filter (Millipore, UK). To remove viral titer
306 bias between different PV stocks, pseudotypes were concentrated and (re-) titrated by serial
307 dilution. Concentration was carried out by ultra-centrifugation for 2 h at 25,000 rpm, 4°C in
308 the SW32 rotor of a L2-65B Beckman ultra-centrifuge.
309 Two-fold serial dilutions of PV-containing supernatant were performed as previously
310 described³² using white 96-well Nunclon[®] plates (Thermo Fisher Scientific, UK).

311 Subsequently, approximately 1×10^4 (for adherent) and 3×10^4 cells (for suspension) cells were
312 added in 50 μ l of medium per well. Plates were incubated for 48 h, after which 50 μ l of
313 Bright-Glo™ substrate (Promega, UK) was added. Luciferase readings were conducted with a
314 luminometer (FLUOstar OPTIMA, BMG Labtech) after a 5-minute incubation period and
315 luciferase reading recorded in relative luminescence units (RLU). Data were normalized using
316 Δ -env and cell-only measurements and expressed as RLU/ml.

317 **Plasmids and transfections**

318 Mammalian expression plasmids (pcDNA3.1+/C-(K)DYK) for HLA-DRA (NM_019111) and
319 HLA-DRB1 (NM_001243965) were purchased from GenScript (Piscataway, NJ; USA).
320 HEK293T/17 cells at sub-confluence in 6-well plates or 100 mm dishes were transfected
321 with HLA-DRA plasmid or HLA-DRB1 plasmid or a 1:1 combination of both using the
322 Lipofectamine 3000 transfection reagent (Thermo Fisher Scientific, UK) according to
323 manufacturer instructions. 48 h after transfection, cells were used either for
324 immunofluorescence analysis, or for FACS analysis (cell-surface staining) or for infection
325 with PV. Under the experimental conditions, the transfection efficiency in either plate/dish,
326 as assessed by the GFP expression of a co-transfected GFP-expressing control plasmid, was
327 >70% under microscopic observation. For HLA-DR stably over expressing cells, PakiTO3
328 cells were transfected with both HLA-DR plasmids and then selected with neomycin (500
329 μ g/ml). Single clones were analysed for expression of the over expressed proteins.

330 **RNA isolation for microarray analysis**

331 Total RNA was isolated from biological triplicates of early and late passage MDCK from T25
332 flasks that had been seeded with 8×10^5 cells and allowed to become confluent and polarize
333 over 4 days in culture cells using a Ribopure kit (Ambion, Austin, TX). Acquired RNA was
334 precipitated with EtOH and subsequently purified employing columns, procedures and
335 reagents from an RNEasy kit (Qiagen, Germantown, MD) and resuspended in RNase-free H₂O.
336 Complementary DNA and RNA synthesis were performed according to Affymetrix Expression

337 Analysis protocols (see www.affymetrix.com). Briefly, double-stranded cDNA was synthesized
338 from 5 µg of total RNA using the Superscript double-stranded cDNA synthesis kit (Invitrogen).
339 Following phenol/chloroform extraction and ethanol precipitation, a biotin-labeled in-vitro
340 transcription reaction was carried out using the cDNA template (Enzo Life Sciences,
341 Farmingdale, NY). Fifteen micrograms of cRNA was fragmented for hybridization to
342 Affymetrix Canine Genome 2.0 Array GeneChips (Santa Clara, CA), which contains
343 approximately 18,000 *C. familiaris* mRNA/EST-based transcripts and over 20,000 non-
344 redundant predicted genes. An one-way ANOVA adjusted with the Benjamini–Hochberg
345 multiple-testing correction [false discovery rate (FDR) of $P < 0.05$] was performed with Partek
346 Genomics Suite (v6.6 Partek) across all samples as previously⁵⁷. Principal component analysis
347 confirmed that batch mixing had prevented introduction of experimental bias. Comparisons
348 were conducted between early and late passaged cells. The analysis cut off criteria were fold
349 change $\geq \pm 1.5$ and P -value ≤ 0.05 . Microarray data was uploaded per MIAME standards and
350 deposited at the GEO repository and is available under series record number GSE14837.

351

352 **HLA-DRA knockdown and blocking using siRNA and monoclonal antibodies**

353 A Sigma-Aldrich MISSION esiRNA endonuclease-derived mixture of siRNAs (EHU226621) was
354 used to knock down HLA-DRA expression in Raji cells. Lipofectamine RNAiMAX transfection
355 Reagent (Thermo Fisher Scientific, UK) was used to transfect exponentially grown Raji cells
356 with 50 nM of siHLA-DRA or siRNA universal negative control (Sigma-Aldrich, UK; SIC001)
357 according to the manufacturer's instructions. The transfection was repeated the following day
358 and cells were collected after 48 h and either seeded at 3×10^4 cells per well in a 96 well-plate
359 for infection with PV or processed in order to validate siRNA activity. Total RNA and protein
360 were collected and assessed by quantitative RT-PCR and western blot, respectively.

361 In order to evaluate the interaction of HLA-DR with H17 we used the HLA DRA mAb
362 (302CT2.3.2), which is generated from mice immunized with a KLH conjugated synthetic

363 peptide between 48-75 amino acids from human HLA-DRA. After a 1 h pre-incubation with
364 increasing concentrations of the antibody in normal growth media, Raji cells (3×10^4) were
365 infected for 24-48 h with H17-or VSV-G-PV.

366

367 **Western blot analysis**

368 Washed cells were lysed on ice with lysis buffer [0.5% NP40 in PBS with 10 mM Tris-HCl, pH
369 7.4 supplemented with Halt Protease Inhibitor mixture EDTA-free (Thermo Fisher Scientific
370 UK)] and protein was quantified by the BCA assay kit (Thermo Fisher Scientific, UK). 20-50 μ g
371 of protein was electrophoresed on a 4-15% sodium dodecylsulfate polyacrylamide gel,
372 alongside a protein ladder (Precision Plus Protein Dual Colour Standards, Bio-Rad) and
373 immunoblotted with the following antibodies using standard procedures: mouse monoclonal
374 anti-HLA-DRA (1:1000; Clone: 302CT2, Enzo Life Sciences, UK) or rabbit monoclonal α -tubulin
375 (1:2000; Cell signalling Technology, UK) antibodies. The membranes were then washed with
376 PBS for three times and incubated with goat anti-rabbit or donkey anti-mouse secondary
377 antibodies (LI-COR) in the dark for 1 h. Scanning was then carried out using the Odyssey
378 Imaging system (LI-COR).

379

380 **Immunofluorescence**

381 Transfected cells with HLA-DRA and -DRB1 expression plasmids or with the empty plasmid
382 were seeded onto glass cover slips at 5×10^4 cells/ml in 6 well plates overnight and were fixed
383 with 4% paraformaldehyde in PBS for 30 minutes at room temperature (RT). Fixed cells were
384 washed with PBS and permeabilised with 1% Triton X-100 in PBS for 10 minutes. After
385 washing with PBS, the cover slips were incubated with a mouse HLA-DRA mAb (169-1B5.2;
386 Bio-Techne Ltd) targeting a monomorphic general framework determinant of HLA-DR Class II
387 antigen, diluted in 5% BSA/PBS for 1 hr at RT. The cover slips were then washed 3X with
388 0.02% Tween 20 and 1% BSA in PBS, followed by incubation with Alexafluor 488 conjugated

389 anti-mouse (Thermo Fisher Scientific, UK) for 30 minutes at RT. After washing 3X with 0.02%
390 Tween 20 and 1% BSA in PBS, the cover slips were mounted using Prolong Gold containing
391 DAPI (Invitrogen). Images were acquired on EVOS fluorescent microscope (EVOS FL imaging
392 system; Life Technology, USA). Experiments were carried out twice.

393

394 **Flow cytometry**

395 For surface staining, human cancer cells and HEK293T/17 cells transfected with an empty
396 vector or expression plasmids of HLA-DR (α and β) chains were maintained in the dark at 4°C
397 throughout. Cells were collected, washed twice in ice-cold FACS buffer (2%FCS, 0.02% NaN₃
398 in PBS) and stained with a FITC-conjugated anti-human HLA-DR mAb (Clone Tü36; BD
399 Biosciences). This antibody specifically binds to a monomorphic epitope of the HLA-DR $\alpha\beta$
400 complex and not the isolated α or β chains or the HLA-DP and -DQ isotypes⁴¹. The cells were
401 analyzed with BD LSR Fortessa to determine expression of HLA-DR in combination with the
402 matched isotype control and sorted into HLA-DR⁻ and HLA-DR⁺ subpopulations with a FACS
403 Aria cell sorter (BDIS, San Jose, CA, USA). The Hoechst 33342 stain was used for cell viability
404 discrimination and the data files were analyzed using the FlowJo software (Tree Star, Inc., Sac
405 Carlos, CA, USA). Data are representative of two independent experiments.

406

407 **Relative and absolute mRNA quantification**

408 qRT-PCR was performed on RNA samples using a two-step procedure. RNA was first reverse-
409 transcribed into cDNA using the QuantiTect Reverse Transcription Kit (Qiagen) according to
410 manufacturer's instructions. qRT-PCR was then conducted on the cDNA in a 384-well plate
411 with a ABI-7900HT Fast qRT-PCR system (Applied Biosystems). Mesa Green qRT-PCR
412 MasterMix (Eurogentec) was added to the cDNA (5 μ l for every 2 μ l of cDNA). The following
413 primers were used: for canine DLA-DRA (Forward: 5'-GCTGTGGACAAAGCTAACCTTG-3',
414 Reverse: 5'-TCTGGAGGTACATTGGTGTTCG-3'), for canine DLA-DRB1 (Forward: 5'-

415 AGCACCAAGTTTGACAAGC-3', Reverse: 5-AAGAGCAGACCCAGGACAAAG-3'). The following
416 amplification conditions were used: 95°C for 5 minutes; 40 cycles of 95°C for 15 seconds, 57°C
417 for 20 seconds, and 72°C for 20 seconds; 95°C for 15 seconds; 60°C for 15 seconds; and 95°C
418 for 15 seconds. The output Ct values and dissociation curves were analysed using SDS v2.3
419 and RQ Manager v1.2 (Applied Biosystems). Gene expression data were normalized against
420 the housekeeping gene GAPDH, and compared with the mock controls using the comparative
421 C_T method (also referred to as the 2^{-ΔΔCT} method⁵⁸). Absolute copy numbers of HLA-DRA in
422 human cell lines were calculated using a standard curve of known concentrations of the
423 corresponding HLA-DRA cDNA expression plasmid. HLA-DRA (Forward: 5'-
424 TCAAGGGATTGCGCAAAGC-3' and reverse 5'- ACACCATCACCTCCATGTGC-3'. All experiments
425 were carried out in triplicate.

426

427 **Prediction of transmembrane protein domains and subcellular topology and** 428 **phylogenetic analysis**

429 For each of the differentially regulated transcripts identified by microarrays, we used Phobius
430 (<http://phobius.sbc.su.se>)⁵⁹ and TMHMM v2.0 (<http://www.cbs.dtu.dk/services/TMHMM/>)⁶⁰
431 to predict the existence of transmembrane protein domains. Similarly, we used Deeploc-1.0
432 (<http://www.cbs.dtu.dk/services/DeepLoc/>)⁶¹ to determine sub-cellular localisation of the
433 encoded proteins. These predictions were compared with gene annotations and literature
434 references to confirm their reliability. The amino acid sequences of canine DLA-DRA
435 (NP_001011723.1), human HLA-DRA (NP_061984.2), and their bat orthologues [*Pteropus*
436 *alecto* (XP_006907484.1) and *Desmodus rotundus* (XP_024413747.1)] were subjected to
437 multiple alignment using CLC workbench 7 (CLC Bio, Qiagen, Aarhus, Denmark).

438

439 **Ethics statement**

440 The buffy coat residues for the isolation of CD19⁺ primary B cells were purchased from the UK
441 Blood Transfusion Service from anonymous volunteers blood donors. Therefore, no ethical
442 approval is required.

443

444 **Statistical Analyses**

445 Graphical representation and statistical analyses were performed using Prism 8 software
446 (GraphPad). Unless otherwise stated, results are shown as means \pm SEM from three
447 independent experiments. Differences were tested for statistical significance using one-way
448 ANOVA with a Dunnett's or a Tukey *posthoc* test. All statistical analyses were two-sided, and p
449 <0.05 was considered statistically significant.

450

451 **Acknowledgements:**

452 Our thanks go to Jim Kaufman, Yanping Guo, Rob White, Amr Bayoumy, Ibrahim Elbusifi,
453 Daragh Quinn and Alfred Ho for their technical assistance. This research was undertaken with
454 the financial support of the Biotechnology and Biological Sciences Research Council (BBSRC)
455 (<http://www.bbsrc.ac.uk>) via Strategic LoLa grant BB/K002465/1 "Developing Rapid
456 Responses to Emerging Virus Infections of Poultry (DRREVIP)" and the Octoberwoman
457 Foundation.

458

459 **References:**

- 460 1. Tong S, *et al.* A distinct lineage of influenza A virus from bats. *Proc Natl Acad Sci U S A*
461 **109**, 4269-4274 (2012).
462
- 463 2. Tong S, *et al.* New world bats harbor diverse influenza A viruses. *PLoS Pathog* **9**,
464 e1003657 (2013).
465
- 466 3. Kandeil A, *et al.* Isolation and characterization of a distinct influenza A virus from
467 Egyptian bats. *J Virol*, (2018).
468
- 469 4. Brunotte L, Beer M, Horie M, Schwemmler M. Chiropteran influenza viruses: flu from
470 bats or a relic from the past? *Curr Opin Virol* **16**, 114-119 (2016).

- 471
472 5. Simonsen L. The global impact of influenza on morbidity and mortality. *Vaccine* **17**
473 **Suppl 1**, S3-10 (1999).
474
475 6. Long JS, Mistry B, Haslam SM, Barclay WS. Host and viral determinants of influenza A
476 virus species specificity. *Nat Rev Microbiol*, (2018).
477
478 7. Gamblin SJ, Skehel JJ. Influenza hemagglutinin and neuraminidase membrane
479 glycoproteins. *J Biol Chem* **285**, 28403-28409 (2010).
480
481 8. Bertram S, Glowacka I, Steffen I, Kuhl A, Pohlmann S. Novel insights into proteolytic
482 cleavage of influenza virus hemagglutinin. *Rev Med Virol* **20**, 298-310 (2010).
483
484 9. Lakadamyali M, Rust MJ, Zhuang X. Endocytosis of influenza viruses. *Microbes Infect* **6**,
485 929-936 (2004).
486
487 10. Sauter NK, *et al.* Hemagglutinins from two influenza virus variants bind to sialic acid
488 derivatives with millimolar dissociation constants: a 500-MHz proton nuclear
489 magnetic resonance study. *Biochemistry* **28**, 8388-8396 (1989).
490
491 11. Edinger TO, Pohl MO, Stertz S. Entry of influenza A virus: host factors and antiviral
492 targets. *J Gen Virol* **95**, 263-277 (2014).
493
494 12. Harrison SC. Viral membrane fusion. *Nat Struct Mol Biol* **15**, 690-698 (2008).
495
496 13. Air GM, Laver WG. The neuraminidase of influenza virus. *Proteins* **6**, 341-356 (1989).
497
498 14. Matrosovich MN, Matrosovich TY, Gray T, Roberts NA, Klenk HD. Neuraminidase is
499 important for the initiation of influenza virus infection in human airway epithelium. *J*
500 *Virol* **78**, 12665-12667 (2004).
501
502 15. Sun X, *et al.* Bat-derived influenza hemagglutinin H17 does not bind canonical avian or
503 human receptors and most likely uses a unique entry mechanism. *Cell Rep* **3**, 769-778
504 (2013).
505
506 16. Li Q, *et al.* Structural and functional characterization of neuraminidase-like molecule
507 N10 derived from bat influenza A virus. *Proc Natl Acad Sci U S A* **109**, 18897-18902
508 (2012).
509
510 17. Zhu X, *et al.* Crystal structures of two subtype N10 neuraminidase-like proteins from
511 bat influenza A viruses reveal a diverged putative active site. *Proc Natl Acad Sci U S A*
512 **109**, 18903-18908 (2012).
513
514 18. Wu Y, Wu Y, Tefsen B, Shi Y, Gao GF. Bat-derived influenza-like viruses H17N10 and
515 H18N11. *Trends Microbiol* **22**, 183-191 (2014).
516
517 19. Maruyama J, *et al.* Characterization of the glycoproteins of bat-derived influenza
518 viruses. *Virology* **488**, 43-50 (2016).
519
520 20. Garcia-Sastre A. The neuraminidase of bat influenza viruses is not a neuraminidase.
521 *Proc Natl Acad Sci U S A* **109**, 18635-18636 (2012).

522

523 21. Cimini K, Thamamongood T, Zimmer G, Schwemmler M. Novel insights into bat
524 influenza A viruses. *J Gen Virol* **98**, 2393-2400 (2017).

525

526 22. Mehle A. Unusual influenza A viruses in bats. *Viruses* **6**, 3438-3449 (2014).

527

528 23. Juozapaitis M, *et al.* An infectious bat-derived chimeric influenza virus harbouring the
529 entry machinery of an influenza A virus. *Nat Commun* **5**, 4448 (2014).

530

531 24. Hoffmann M, Kruger N, Zmora P, Wrensch F, Herrler G, Pohlmann S. The
532 Hemagglutinin of Bat-... *PLoS One* **11**, e0152134 (2016).

533

534 25. Zhou B, *et al.* Characterization of uncultivable bat influenza virus using a replicative
535 synthetic virus. *PLoS Pathog* **10**, e1004420 (2014).

536

537 26. Moreira EA, *et al.* Synthetically derived bat influenza A-like viruses reveal a cell type-
538 but not species-specific tropism. *Proc Natl Acad Sci U S A* **113**, 12797-12802 (2016).

539

540 27. Carnell GW, Ferrara F, Grehan K, Thompson CP, Temperton NJ. Pseudotype-based
541 neutralization assays for influenza: a systematic analysis. *Front Immunol* **6**, 161 (2015).

542

543 28. Li Q, Liu Q, Huang W, Li X, Wang Y. Current status on the development of
544 pseudoviruses for enveloped viruses. *Rev Med Virol* **28**, (2018).

545

546 29. King B, Daly J. Pseudotypes: your flexible friends. *Future Microbiol* **9**, 135-137 (2014).

547

548 30. Coakley E, Petropoulos CJ, Whitcomb JM. Assessing chemokine co-receptor usage in
549 HIV. *Curr Opin Infect Dis* **18**, 9-15 (2005).

550

551 31. Cronin J, Zhang XY, Reiser J. Altering the tropism of lentiviral vectors through
552 pseudotyping. *Curr Gene Ther* **5**, 387-398 (2005).

553

554 32. Carnell G, *et al.* The bat influenza H17N10 can be neutralized by broadly- neutralizing
555 monoclonal antibodies and its neuraminidase can facilitate viral egress. bioRxiv
556 499947; doi: <https://doi.org/10.1101/499947> (2018).

557

558 33. Dukes JD, Whitley P, Chalmers AD. The MDCK variety pack: choosing the right strain.
559 *BMC Cell Biol* **12**, 43 (2011).

560

561 34. Nowak SA, Chou T. Mechanisms of receptor/coreceptor-mediated entry of enveloped
562 viruses. *Biophys J* **96**, 2624-2636 (2009).

563

564 35. Byrd-Leotis L, Cummings RD, Steinhauer DA. The interplay between the host receptor
565 and influenza virus hemagglutinin and neuraminidase. *Int J Mol Sci* **18**, (2017).

566

567 36. Kaufman JF, Auffray C, Korman AJ, Shackelford DA, Strominger J. The class II molecules
568 of the human and murine major histocompatibility complex. *Cell* **36**, 1-13 (1984).

569

570 37. Blazekovic F, *et al.* HLA-DR peptide occupancy can be regulated with a wide variety of
571 small molecules. *Hum Vaccin Immunother* **12**, 593-598 (2016).

572

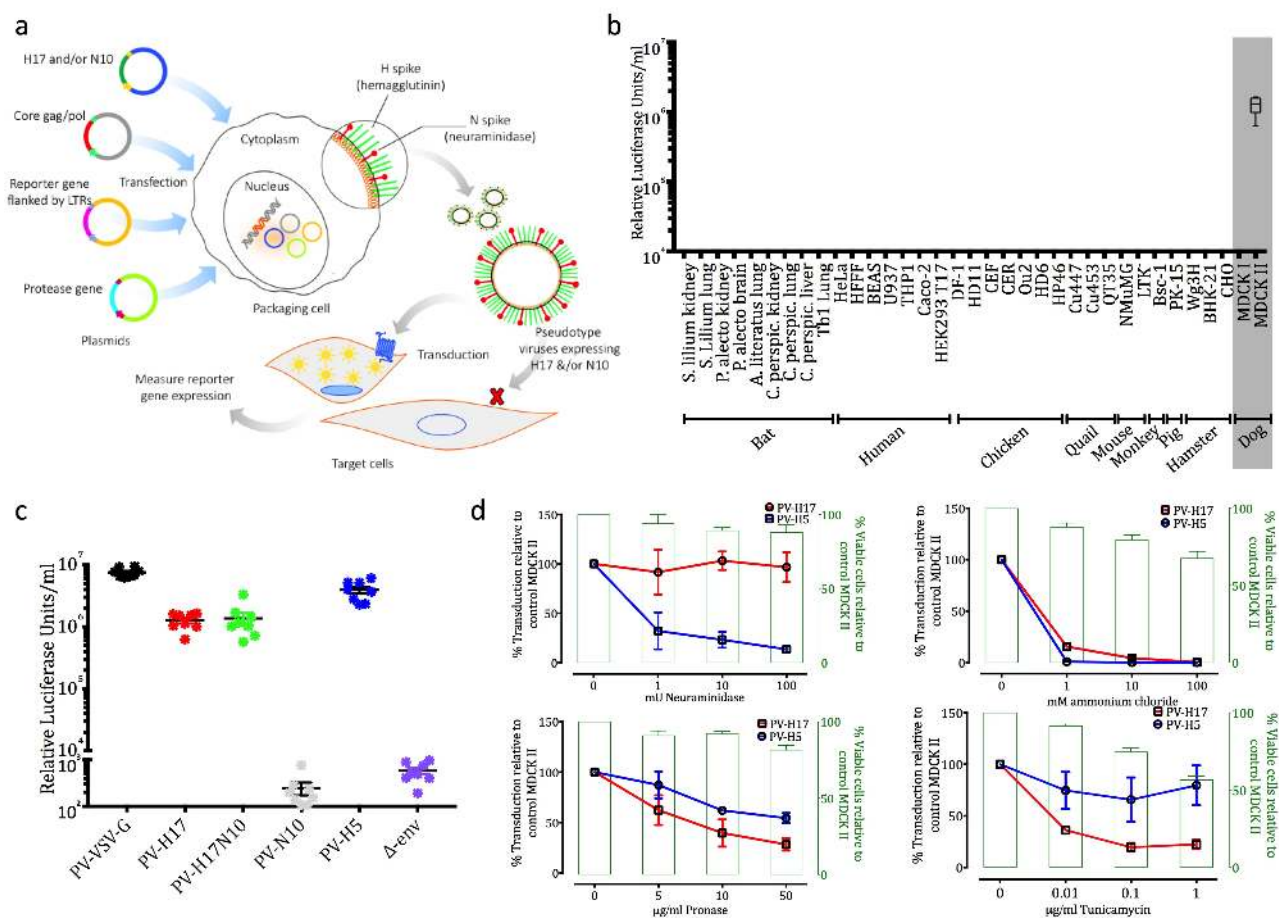
- 573 38. Jones EY, Fugger L, Strominger JL, Siebold C. MHC class II proteins and disease: a
574 structural perspective. *Nat Rev Immunol* **6**, 271-282 (2006).
575
- 576 39. Roche PA, Furuta K. The ins and outs of MHC class II-mediated antigen processing and
577 presentation. *Nat Rev Immunol* **15**, 203-216 (2015).
578
- 579 40. Nagy ZA, *et al.* Fully human, HLA-DR-specific monoclonal antibodies efficiently induce
580 programmed death of malignant lymphoid cells. *Nat Med* **8**, 801-807 (2002).
581
- 582 41. Ziegler A, *et al.* Analysis by sequential immunoprecipitations of the specificities of the
583 monoclonal antibodies TU22, 34, 35, 36, 37, 39, 43, 58 and YD1/63. HLK directed
584 against human HLA class II antigens. *Immunobiology* **171**, 77-92 (1986).
585
- 586 42. Watanabe N, *et al.* A cell-based high-throughput screening assay system for inhibitor
587 compounds of antigen presentation by HLA class II molecule. *Sci Rep* **7**, 6798 (2017).
588
- 589 43. van Lith M, McEwen-Smith RM, Benham AM. HLA-DP, HLA-DQ, and HLA-DR have
590 different requirements for invariant chain and HLA-DM. *J Biol Chem* **285**, 40800-40808
591 (2010).
592
- 593 44. Grove J, Marsh M. The cell biology of receptor-mediated virus entry. *J Cell Biol* **195**,
594 1071-1082 (2011).
595
- 596 45. Stamatakis Z, *et al.* Hepatitis C virus association with peripheral blood B lymphocytes
597 potentiates viral infection of liver-derived hepatoma cells. *Blood* **113**, 585-593 (2009).
598
- 599 46. Lemon K, *et al.* Early target cells of measles virus after aerosol infection of non-human
600 primates. *PLoS Pathog* **7**, e1001263 (2011).
601
- 602 47. Shannon-Lowe CD, Neuhierl B, Baldwin G, Rickinson AB, Delecluse HJ. Resting B cells
603 as a transfer vehicle for Epstein-Barr virus infection of epithelial cells. *Proc Natl Acad
604 Sci U S A* **103**, 7065-7070 (2006).
605
- 606 48. Rensing ME, *et al.* Interference with T cell receptor-HLA-DR interactions by Epstein-
607 Barr virus gp42 results in reduced T helper cell recognition. *Proc Natl Acad Sci U S A*
608 **100**, 11583-11588 (2003).
609
- 610 49. Rensing ME, *et al.* Epstein-Barr virus gp42 is posttranslationally modified to produce
611 soluble gp42 that mediates HLA class II immune evasion. *J Virol* **79**, 841-852 (2005).
612
- 613 50. Wiertz EJ, Devlin R, Collins HL, Rensing ME. Herpesvirus interference with major
614 histocompatibility complex class II-restricted T-cell activation. *J Virol* **81**, 4389-4396
615 (2007).
616
- 617 51. Jeffers SA, *et al.* CD209L (L-SIGN) is a receptor for severe acute respiratory syndrome
618 coronavirus. *Proc Natl Acad Sci U S A* **101**, 15748-15753 (2004).
619
- 620 52. Li W, *et al.* Angiotensin-converting enzyme 2 is a functional receptor for the SARS
621 coronavirus. *Nature* **426**, 450-454 (2003).
622

- 623 53. Ferrara F, *et al.* The human Transmembrane Protease Serine 2 is necessary for the
624 production of Group 2 influenza A virus pseudotypes. *J Mol Genet Med* **7**, 309-314
625 (2012).
626
- 627 54. Zufferey R, Nagy D, Mandel RJ, Naldini L, Trono D. Multiply attenuated lentiviral vector
628 achieves efficient gene delivery in vivo. *Nat Biotechnol* **15**, 871-875 (1997).
629
- 630 55. Demaison C, *et al.* High-level transduction and gene expression in hematopoietic
631 repopulating cells using a human immunodeficiency virus type 1-based lentiviral
632 vector containing an internal spleen focus forming virus promoter. *Hum Gene Ther* **13**,
633 803-813 (2002).
634
- 635 56. Cox RJ, Mykkeltvedt E, Robertson J, Haaheim LR. Non-lethal viral challenge of influenza
636 haemagglutinin and nucleoprotein DNA vaccinated mice results in reduced viral
637 replication. *Scand J Immunol* **55**, 14-23 (2002).
638
- 639 57. Giotis ES, Ross CS, Robey RC, Nohturfft A, Goodbourn S, Skinner MA. Constitutively
640 elevated levels of SOCS1 suppress innate responses in DF-1 immortalised chicken
641 fibroblast cells. *Sci Rep* **7**, 17485 (2017).
642
- 643 58. Pfaffl MW. A new mathematical model for relative quantification in real-time RT-PCR.
644 *Nucleic Acids Res* **29**, e45 (2001).
645
- 646 59. Kall L, Krogh A, Sonnhammer EL. Advantages of combined transmembrane topology
647 and signal peptide prediction--the Phobius web server. *Nucleic Acids Res* **35**, W429-
648 432 (2007).
649
- 650 60. Krogh A, Larsson B, von Heijne G, Sonnhammer EL. Predicting transmembrane protein
651 topology with a hidden Markov model: application to complete genomes. *J Mol Biol*
652 **305**, 567-580 (2001).
653
- 654 61. Almagro Armenteros JJ, Sonderby CK, Sonderby SK, Nielsen H, Winther O. DeepLoc:
655 prediction of protein subcellular localization using deep learning. *Bioinformatics* **33**,
656 4049 (2017).
657
658
659
660

661 **Figure legends:**

662 **Figure 1: a.** Schematic representation of pseudotype virus production. Expression plasmids
663 for the HIV-1 gag-pol gene, the bat H17 alone or with N10, the luciferase reporter gene with
664 HIV-1 long tandem repeats (LTRs) and the protease gene (HAT or TMPRSS2) are generated
665 and co-transfected into producer HEK293T/17 cells. Cells transcribe and translate the HIV-1
666 core genes, BatIV glycoproteins are packaged on the cell surface, and viruses bud off in an
667 HIV-1 dependent manner. Production of N10-PV does not require co-transfection with a

668 protease gene. Supernatants are harvested at 48 h post-transfection and the produced
 669 pseudotype viruses (PVs) are filtered, titrated and infected into target cells. **b.** Infectivity
 670 titers of H17-PV in cells from different tissues/species [expressed in Relative Luciferase Units
 671 (RLU)/ml]. Mean luciferase activity was plotted as mean \pm inter-assay deviation expressed as
 672 SEM from 3-6 independent experiments. **c.** Infectivity titers of H17-PV, N10 and control
 673 pseudotypes (VSV-G, H5 and Δ -env) in MDCK II cells. **d.** MDCK II cells were pre-treated with
 674 either neuraminidase (2 h), with pronase (30 mins) or tunicamycin (5 h) or treated with
 675 ammonium chloride, and then infected with H17-PV. Luciferase activities were measured
 676 after 24 h with a luminometer. The left Y-axis shows infection levels (% of control) and the
 677 right Y-axis shows % viability of cells related to control MDCK II cells. Experiments were
 678 carried out in triplicate.



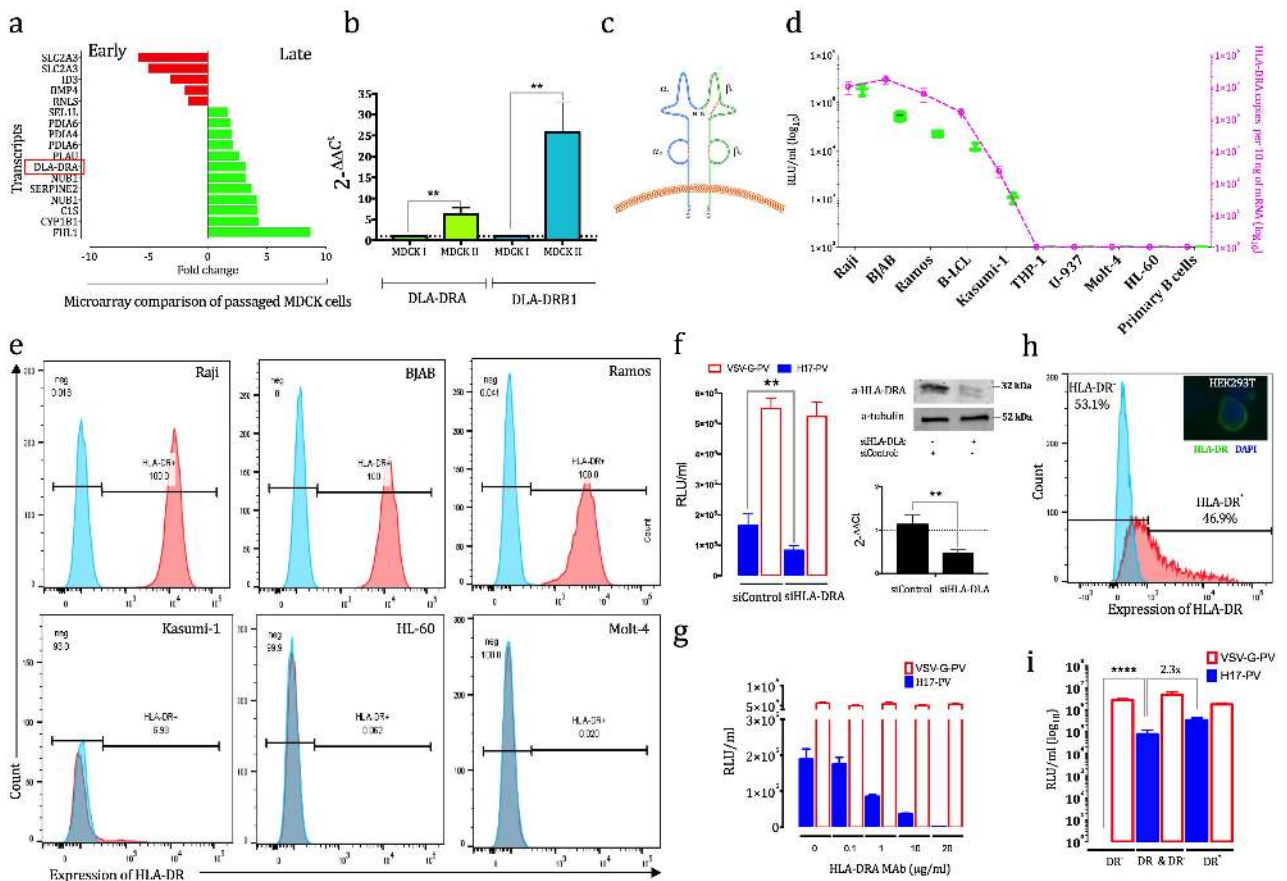
679

680

681

682 **Figure 2: a.** Significantly expressed genes in the microarray comparison of late versus early
683 passaged MDCK cells (green and red columns represent upregulated transcripts in MDCK II
684 and MDCK I cells respectively). Analysis was conducted with Partek (fold change ≥ 1.5 and
685 $FDR \leq 0.05$). Red frame indicates the transcript upregulated in late passaged MDCK cells
686 encoding a membrane protein. **b.** qRT-PCR results showing the expression of DLA-DRA and
687 DLA-DRB1 mRNA in MDCK I and II cells. The data are expressed as the means \pm S.E.M. from
688 three independent experiments. One-way Anova with Tukey *posthoc* test were used to analyse
689 the data. $**P < 0.005$ versus control. **c.** Schematic diagram of the MHC II surface molecules. **d.**
690 Left Y-axis (green box and whiskers): relative infection titers of H17-PV [\log_{10} Relative
691 Luciferase Units (RLU) /ml] in a panel of human cancer cell lines. Right Y-axis (broken purple
692 line) shows \log_{10} HLA-DRA mRNA copies with qRT-PCR. The data are expressed as the means
693 \pm S.E.M. from three independent experiments. **e.** FACS analysis of the expression levels of cell-
694 surface HLA-DR molecule from three H17-PV susceptible and three unsusceptible cancer cell
695 lines. Results are representative from two independent experiments. Blue and red peaks
696 represent HLA-DR⁻ and HLA-DR⁺ subpopulations respectively. **f.** Left: infection titers of VSV-G-
697 and H17-PV (RLU/ml) in Raji cells transfected with siControl or siHLA-DRA. Right: western
698 blot (top) and qRT-PCR (bottom) showing expression of HLA-DRA protein and mRNA in
699 transfected Raji with siRNA versus siControl. Experiments were carried out twice and the
700 data are expressed as means \pm S.E.M. One-way Anova with Dunnett *posthoc* test were used to
701 analyse the data. $**P < 0.005$ versus siControl. **g.** Relative infection titers of VSV-G- and H17-PV
702 (RLU/ml) in Raji cells incubated with different concentrations of a monoclonal antibody
703 targeting HLA-DRA. The data are expressed as the means \pm S.E.M. from three independent
704 experiments. **h.** FACS analysis of the expression levels of cell-surface HLA-DR heterodimer in
705 transiently transfected HEK293T/17 cells for 48 h with expression vectors for DRA and DRB1
706 (1:1 ratio). Right hand corner microscopy picture (80x) shows immunofluorescence
707 confirming surface expression of HLA-DR on cells (green stain: FITC-HLA-DR and blue: DAPI).

708 The data are representative from two independent experiments. **i.** Relative infection titers of
 709 VSV-G- and H17-PV [in log₁₀ Relative Luciferase Units (RLU) /ml] in FACS-sorted DR-
 710 HEK293T/17 cells, unsorted transiently transfected (DR⁺ & DR⁻) and FACS-sorted DR⁺ cells.
 711 Experiments were carried out twice and the data are expressed as the means ± S.E.M. One-
 712 way Anova with Dunnett *posthoc* test were used to analyse the data. ***P*<0.005 versus DR-
 713 cells.



714

715

716

717

718

719

720

721

722 **Supplementary material**

723 **Supplementary Material 1: List of cell lines included in the study.**

| Cell line | Type of cells | Species | Origin |
|---------------------------|-----------------------------------|-------------------------------|---|
| Raji | Burkitt's lymphoma mature B-cells | Human | ATCC CCL-86 |
| Ramos | Burkitt's lymphoma mature B-cells | Human | ATCC CRL-1596 |
| BJAB | Burkitt's lymphoma mature B-cells | Human | CVCL_5711 |
| HL-60 | Promyeloblasts | Human | ATCC CCL-240 |
| Molt-4 | T lymphoblasts | Human | ATCC CRL-1582 |
| Jurkat | T lymphocytes | Human | ATCC TIB-152 |
| U-937 | Monocytic leukemia | Human | ATCC CRL-1593.2 |
| THP-1 | Monocytic lymphoma | Human | ATCC TIB-202 |
| B-LCLs | B-lymphoblastoid | Human | DOI: 10.1093/nar/gkw1167 |
| Kasumi-1 | Myeloblasts | Human | ATCC CRL-2724 |
| Tb1 Lu | Epithelial lung | <i>Tadarida brasiliensis</i> | ATCC CCL-88 |
| <i>S. liliun</i> lung | Lung | <i>Sturnira liliun</i> | Adolfo-Garcia Sastres & Martinez (The Icahn School of Medicine at Mount Sinai, NY, USA)/Aguilera's labs (Univ. of Costa Rica) |
| <i>S. liliun</i> kidney | Kidney | <i>Sturnira liliun</i> | |
| <i>Ar. literatus</i> lung | Lung | <i>Artibeus literatus</i> | |
| <i>C. perspic</i> kidney | Kidney | <i>Carollia perspicillata</i> | |
| <i>C. perspic</i> lung | Lung | <i>Carollia perspicillata</i> | |
| <i>C. perspic</i> liver | Liver | <i>Carollia perspicillata</i> | |
| PakiT03 cells | Epithelial kidney | <i>Pteropus Alecto</i> | Linfa Wang lab, NUS DOI: 10.1371/journal.pone.000826 |
| PaBr cells | Brain | <i>Pteropus Alecto</i> | |
| A549 cells | Epithelial lung | Human | ATCC CRM-CCL-185 |
| BEAS-2B | Epithelial lung/bronchus | Human | ATCC CRL-9609 |
| HFF-1 | Skin fibroblasts | Human | ATCC SCRC-1041 |
| HeLa | Epithelial cervix | Human | ATCC CCL-2 |
| HeLa S3 | Epithelial cervix | Human | ATCC CCL-2.2 |
| Caco-2 | Epithelial colon | Human | ATCC HTB-37 |
| HEK293T17 | Kidney | Human | ATCC CRL-11268 |
| DF-1 | Embryo fibroblast | Chicken | ATCC CRL-12203 |
| HD11 | Macrophages | Chicken | CVCL_4685 |
| CEF | Embryo fibroblasts | Chicken | The Pirbright Institute, UK |
| CER | Embryo-related | Chicken | DOI: 10.1016/j.biologicals.2005.08.001 |
| Ou2 | Fibroblasts | Chicken | CVCL_Y589 |
| HD6 | Erythroblasts | Chicken | PMCID: PMC230774 |

| | | | |
|----------|-----------------------------------|---------|--|
| HP46 | ALV-carcinoma | Chicken | PMCID: PMC361083 |
| Cu447 | Tumor cell line | Quail | DOI: 10.1637/7182-032604R |
| Cu453 | Tumor cell line | Quail | DOI: 10.1637/7182-032604R |
| QT35 | Muscle fibroblasts | Quail | ECACC:93120832 |
| NMuMG | Mammary gland | Mouse | ATCC CRL-1636 |
| LTK-11 | Fibroblasts | Mouse | ATCC CRL-10422 |
| BS-C-1 | Kidney epithelial | Monkey | ATCC CCL 26 |
| PK-15 | Kidney epithelial | Pig | ATCC CCL-33 |
| Wg3HCL2 | HGPRT-Chinese hamster fibroblasts | Hamster | DOI: 10.1186/1297-9686-34-4-521 |
| BHK-21 | Kidney fibroblast | Hamster | ATCC CCL-10 |
| CHO 1-15 | Ovary epithelial | Hamster | ATCC CRL-9606 |
| NBL-2 | Epithelial kidney | Canine | ATCC CCL-34 |
| MDCK I | Epithelial kidney | Canine | EEACC 00062106 |
| MDCK II | Epithelial kidney | Canine | EEACC 00062107 |

724

725

726 **Supplementary Material 2: List of the differentially regulated genes determined by**
727 **microarray comparison between early and late passaged MDCK cells, as summarised in**
728 **Fig. 2a.** The encoded proteins of the differentially regulated transcripts were surveyed for
729 their subcellular localisation (with the DeepLoc server) and presence of transmembrane
730 domains (using the PHOBIUS and TMHMM algorithms).

| Affymetrix ID | Refseq ID | Gene symbol | Gene name | Subcellular localisation (DeepLoc server) | Predicted transmembrane domains | | FDR | Fold change |
|-----------------------|---|-------------|---|---|---------------------------------|----------------|----------|-------------|
| | | | | | TMHMM server | Phobius server | | |
| Cfa.12195.3.S1_at | XM_003435535 XM_005641862 XM_014111636 XM_861215 | FHL1 | Four and a half LIM domains 1 | Nucleus, Soluble | 0 | | 2.63E-05 | 8.68212 |
| CfaAffx.10229.1.S1_at | NM_001159684 | CYP1B1 | Cytochrome P450, family 1, subfamily B, polypeptide 1 | Endoplasmic reticulum, Membrane | 0 | | 1.28E-05 | 4.30944 |
| Cfa.10821.1.A1_s_at | XM_005637210 XM_848227 | C1S | Complement component 1, s subcomponent | Extracellular, Soluble | 0 | | 4.36E-06 | 4.21145 |

| | | | | | | | | |
|----------------------|--|----------|---|--------------------------------|---|---------|----------|---------|
| Cfa.12556.1.A1_at | XM_014119919 | NUB1 | Negative regulator of ubiquitin-like proteins 1 | Cytoplasm, Soluble | 0 | | 2.01E-05 | 4.14298 |
| Cfa.4394.1.S1_at | XM_014111110 | SERPINE2 | Serpin peptidase inhibitor, clade E (nexin, plasminogen activator inhibitor type 1) | Extracellular, Soluble | 0 | | 2.01E-05 | 3.70338 |
| Cfa.7284.1.A1_s_at | XM_014119919 | NUB1 | Negative regulator of ubiquitin-like proteins 1 | Cytoplasm, Soluble | 0 | | 2.21E-05 | 3.22491 |
| Cfa.6456.1.S1_at | NM_001011723 XM_005627066 XM_005627067 | DLA-DRA | MHC class II DR alpha chain | Cell membrane, Membrane | 1 | 221-241 | 2.77E-05 | 3.21344 |
| Cfa.127.1.S1_s_at | NM_001194952 | PLAU | Plasminogen activator, urokinase | Extracellular, Soluble | 0 | 20-40 | 2.14E-05 | 2.69368 |
| CfaAffx.6163.1.S1_at | XM_532876 | PDIA6 | Protein disulfide isomerase family A, member 6 | Endoplasmic reticulum, Soluble | 0 | | 1.83E-05 | 2.10444 |
| Cfa.4275.2.S1_at | XM_843145 | PDIA4 | Protein disulfide isomerase family A, member 4 | Endoplasmic reticulum, Soluble | 1 | | 8.19E-06 | 2.05558 |

| | | | | | | | | |
|-------------------------|---|--------|--|---------------------------------|----|---|----------|--------------|
| CfaAffx.6163.1.S1_s_at | XM_532876 | PDIA6 | Protein disulfide isomerase family A, member 6 | Endoplasmic reticulum, Soluble | 0 | | 8.36E-06 | 1.9391 |
| CfaAffx.26500.1.S1_s_at | XM_014116111 XM_537530 | SEL1L | Sel-1 suppressor of lin-12-like (C. elegans) | Endoplasmic reticulum, Membrane | 1 | 768-786 | 5.15E-06 | 1.69924 |
| Cfa.12560.1.A1_at | XM_005636642 XM_014108134 XM_847958 XR_001314613 XR_001314614 | RNLS | Renalase, FAD-dependent amine oxidase | Mitochondrion, Membrane | 0 | | 3.65E-07 | - 1.64221 |
| CfaAffx.22914.1.S1_at | NM_001287170 | BMP4 | Bone morphogenetic protein 4 | Nucleus, Soluble | 0 | | 2.56E-05 | - 1.93435 |
| Cfa.64.1.S1_at | NM_001003025 | ID3 | Inhibitor of DNA binding 3, dominant negative helix-loop-helix protein | Nucleus, Soluble | 0 | | 3.38E-06 | - 3.17884 |
| Cfa.825.1.S2_at | NM_001003308 | SLC2A3 | Solute carrier family 2 (facilitated glucose transporter), member 3 | Cell membrane, Membrane | 10 | 7-26, 62-85, 97-115, 121-142, 154-177, 183-205, 270-293, 305-326, 333-355, 361-379, 400-420, 426-448 | 6.71E-06 | - 5.03551 |

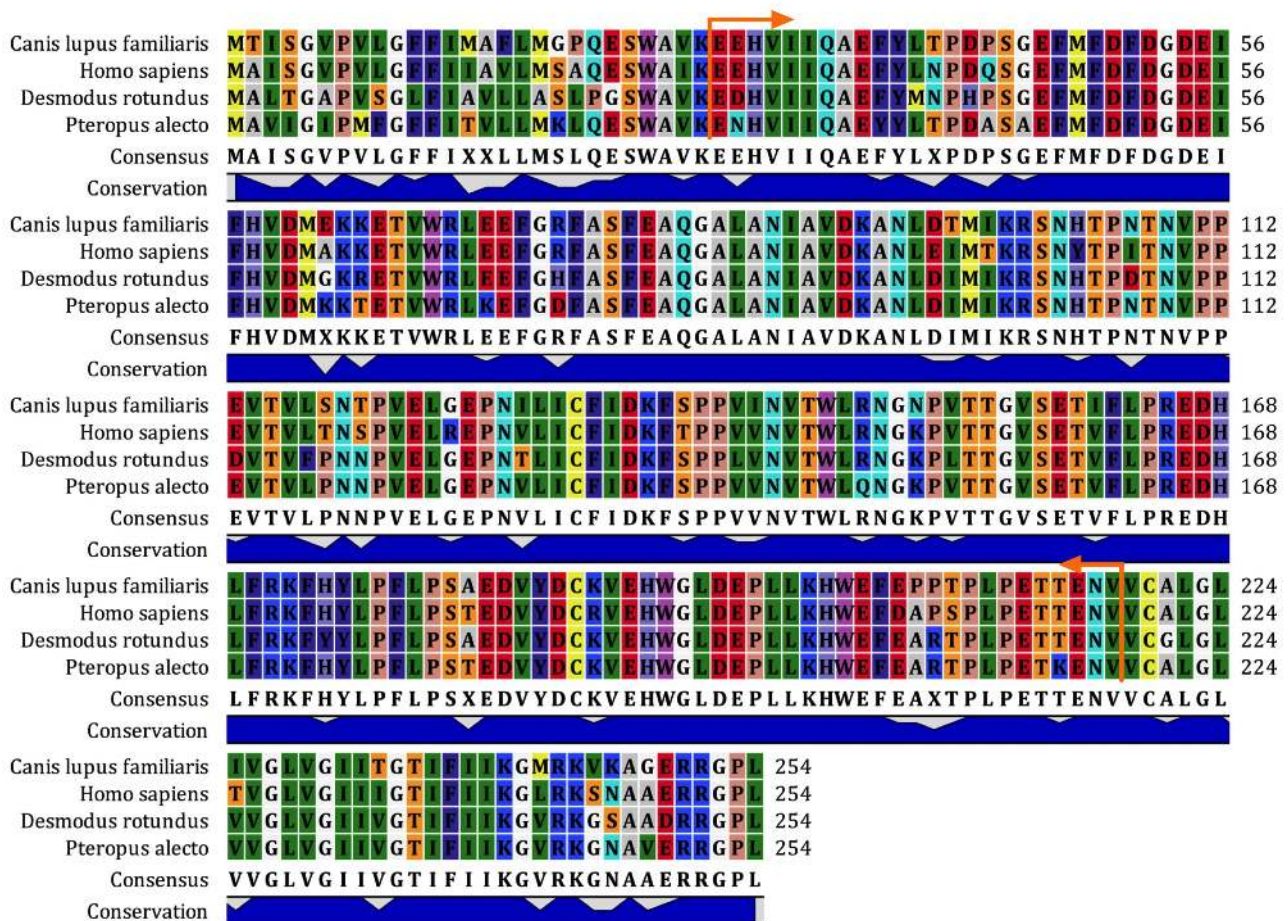
| | | | | | | | | | |
|-----------------------|--------------|--------|---|-------------------------|----|----------|---|---------|--|
| | | | | | | | 7-26, 62-85, 97-115, 121- 142, 154- 177, 183- 205, 270- 293, 305- 326, 333- 355, 361- 379, 400- 420, 426-448 | | |
| CfaAffx.21479.1.S1_at | NM_001003308 | SLC2A3 | Solute carrier family 2 (facilitated glucose transporter), member 3 | Cell membrane, Membrane | 10 | 2.21E-05 | - | 5.89883 | |

731

732

733 **Supplementary Material 3: The ectodomain of HLA-DRA is well conserved in bats,**
734 **humans and canine.**

735 Multiple amino acid sequence alignment of canine DLA-DRA (NP_001011723.1), human HLA-
736 DRA (NP_061984.2), and their bat orthologues [(Yinpterochiroptera *Pteropus alecto*
737 (XP_006907484.1) and Yangochiroptera *Desmodus rotundus* (XP_024413747.1)]. *Desmodus*
738 *rotundus* (common vampire bat) was chosen as the closest species to *Sturnira lilium* with a
739 decoded genome. The alignment was performed by importing the corresponding amino acid
740 sequences into CLC Workbench (CLC Bio, Qiagen, Aarhus, Denmark). Orange arrows indicate
741 the ectodomain of the protein. Matrix below shows overall, pairwise amino acid similarity of
742 HLA-DRA between the four species. The percent amino acid similarity values were calculated
743 with the CLC workbench program.

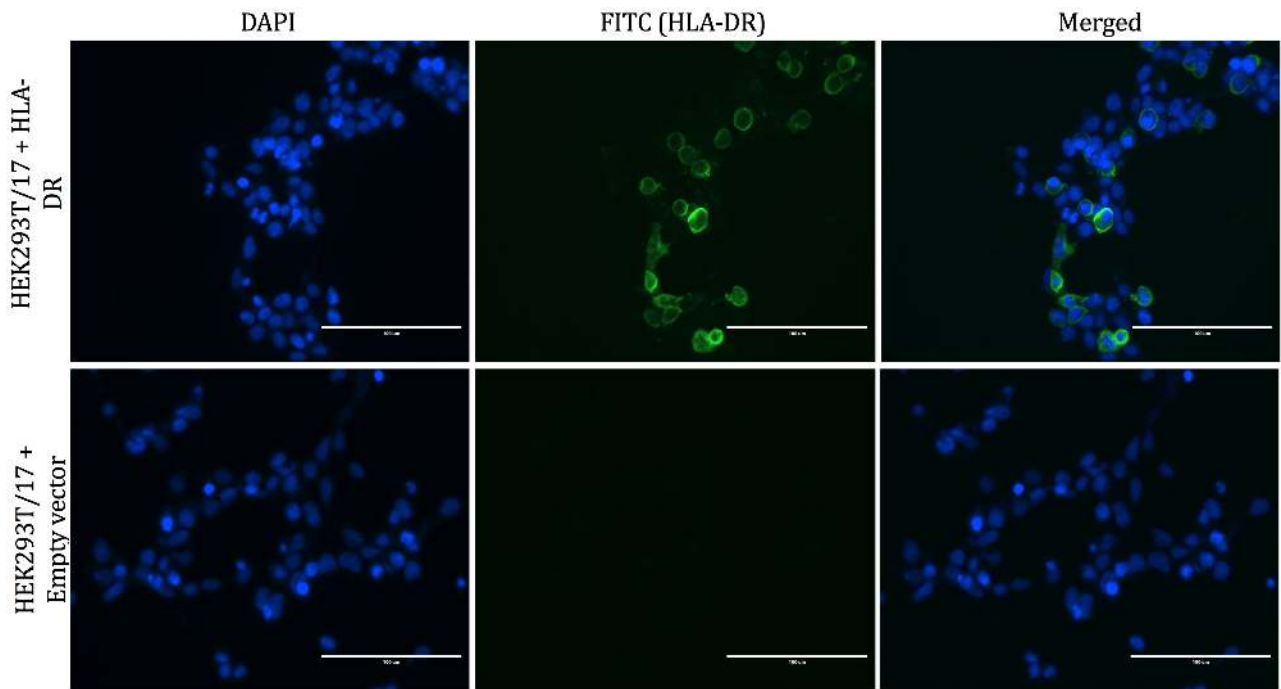


| | 1 | 2 | 3 | 4 |
|------------------------|---|-------|-------|-------|
| Canis lupus familiaris | 1 | 89.01 | 88.48 | 89.53 |
| Homo sapiens | 2 | 89.01 | 86.39 | 87.96 |
| Desmodus rotundus | 3 | 88.48 | 86.39 | 89.01 |
| Pteropus alecto | 4 | 89.53 | 87.96 | 89.01 |

744

745 **Supplementary Material 4: Transfection of HEK293T/17 with HLA-DR α and β chains**
746 **results in surface expression of the heterodimer.**

747 HEK293T/17 cells were transfected with the empty vector or with HLA-DRA and DRB1
748 expression plasmids. The cells were fixed in paraformaldehyde and were permeabilised with
749 Triton X-100 to show intracellular distribution and immuno-stained with mAb HLA-DRA.
750 Nuclei were stained blue with DAPI stain (left panel), HLA-DR heterodimers were stained
751 green (middle panel), and the right panel shows a merged image. Fluorescent microscopy
752 analysis was performed with the EVOS FL fluorescent imaging system. Original magnification,
753 $\times 20$.



754

755 **Supplementary Material 5: Transfection of bat PakiTO3 cells with HLA-DR α and β**
756 **chains confers susceptibility to H17-PV.**

757 Infectivity titers of H17-PV (RLU/ml) in PakiTO3 cells transfected for 48 h with equimolar
758 amounts of either empty vector (pcDNA3.1) or the expression plasmid for HLA-DRA or the
759 expression plasmids encoding both chains of HLA-DR. Cells were infected with PV for an extra
760 72 h in the presence of neomycin. Data represent mean values \pm SEM of three independent
761 experiments. One-way Anova with Dunnett *posthoc* test were used to analyse the data.
762 **** $P < 0.00005$ versus cells transfected with the empty vector.

